

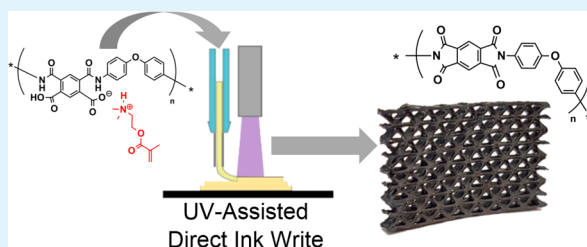
# Ultraviolet-Assisted Direct Ink Write to Additively Manufacture All-Aromatic Polyimides

Daniel A. Rau,<sup>†,‡</sup> Jana Herzberger,<sup>†,§</sup> Timothy E. Long,<sup>§</sup> and Christopher B. Williams<sup>\*‡</sup>

<sup>†</sup>Department of Mechanical Engineering and Macromolecules Innovation Institute (MII) and <sup>§</sup>Department of Chemistry and Macromolecules Innovation Institute (MII), Virginia Tech, Blacksburg, Virginia 24061, United States

 Supporting Information

**ABSTRACT:** All-aromatic polyimides have degradation temperatures above 500 °C, excellent mechanical strength, and chemical resistance, and are thus ideal polymers for high-temperature applications. However, their all-aromatic structure impedes additive manufacturing (AM) because of the lack of melt processability and insolubility in organic solvents. Recently, our group demonstrated the design of UV-curable polyamic acids (PAA), the precursor of polyimides, to enable their processing using vat photopolymerization AM. This work leverages our previous synthetic strategy and combines it with the high solution viscosity of nonisolated PAA to yield suitable UV-curable inks for UV-assisted direct ink write (UV-DIW). UV-DIW enabled the design of complex three-dimensional structures comprising of thin features, such as truss structures. Dynamic mechanical analysis of printed and imidized specimens confirmed the thermomechanical properties typical of all-aromatic polyimides, showing a storage modulus above 1 GPa up to 400 °C. Processing polyimide precursors via DIW presents opportunity for multimaterial printing of multifunctional components, such as three-dimensional integrated electronics.



**KEYWORDS:** direct ink write, UV-DIW, additive manufacturing, Kapton, PMDA-ODA polyimide, polyamic acid salts, 3D printing

Additive manufacturing (AM), or 3D printing processes, create customized, complex three-dimensional components via a layer-wise fabrication approach.<sup>1</sup> Although rapidly growing, industrial adoption of AM is stymied by a limited selection of processable high-temperature engineering polymers.<sup>2</sup> The current library of polymers were optimized for traditional manufacturing processes (e.g., molding and extrusion processes), but are not necessarily well-suited for the unique physics of the layer-by-layer nature of AM processes and their rapid nonhomogeneous kinetics. As such, polymers must be adapted to work within the physics of AM processes. In particular, high-performance polymers need to be modified to be utilized in AM due to their high or nonexistent flow temperatures and low solubility. While researchers developed strategies to 3D print high-performance polymers, such as poly(ether ether ketone) (PEEK),<sup>3</sup> poly(phenylene sulfide),<sup>4</sup> and thermoplastic poly(ether imide)s,<sup>5</sup> sparse attention has been devoted to the AM of all-aromatic, nonmelt processable PIs.<sup>6–8</sup>

Poly(4,4'-oxidiphenylene pyromellitimide) (PMDA-ODA) PI has been developed in the 1960s and is commercially known by the trade name Kapton. It is one of the highest performing polymers due to its excellent mechanical strength over a temperature range of –269 °C to +400 °C.<sup>9</sup> Its all-aromatic chemical structure provides chemical and UV-irradiation resistance and nonflammability, which render it attractive for aerospace and defense applications.<sup>9</sup> Its low dissipation factors and low dielectric constant also make it

well-suited for electronic applications.<sup>9</sup> Although the all-aromatic structure imparts outstanding properties to PMDA-ODA PI, its lack of sufficient melt flow and insolubility in organic solvents precludes traditional manufacturing (e.g., molding, casting, extrusion). Traditionally, PMDA-ODA PI is processed in the nonimidized polyamic acid (PAA) form. PAA is dissolved in an aprotic polar solvent, casted on a substrate and thermally imidized to yield the nonsoluble PI.<sup>10</sup> This solvent-based fabrication pairs the PI parts with an inherent 2D form factor. Three-dimensional PMDA-ODA PI parts are accessible, but require high-temperature sintering processes, which restricts part of the design.<sup>10,11</sup>

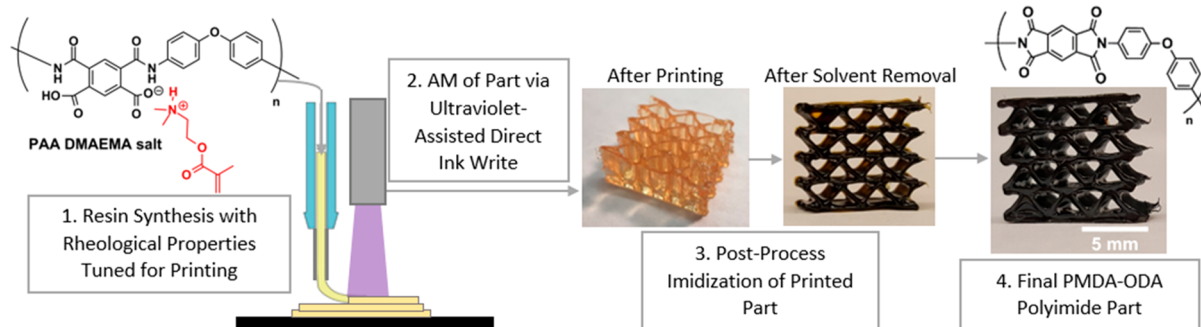
These challenges have made AM of all-aromatic PIs elusive. To date, only few reports have addressed AM of PMDA-ODA PI. One utilized inkjet printing to manufacture thin insulating layers for capacitors, but the process was incapable of forming 3D structures.<sup>8</sup> Our group has modified PMDA-ODA PAA for vat photopolymerization (VP).<sup>6,7</sup> VP, also known as stereolithography, utilizes a vat that is filled with a liquid photoresin. Subsequent patterned UV irradiation selectively cures the photoresin, to create a 3D part layer-by-layer.<sup>12</sup> Inspired by photosensitive polyimides used in photolithographic processes to produce thin patterned films for the microelectronics industry,<sup>13</sup> our group synthesized a resin consisting of a photo-

Received: August 23, 2018

Accepted: October 5, 2018

Published: October 5, 2018

**Scheme 1.** Process Summary of Printing PMDA-ODA PI Parts Starting with the Synthesis of a Tailored UV-Curable Ink (PAA DMAEMA Salt Solution)<sup>a</sup>



<sup>a</sup>Printing using UV-DIW produced a self-supporting 3D organogel structure. Thermal treatment released the solvent, promoted thermal degradation of the PDMAEMA crosslinks, and imidized the ink to yield all-aromatic PMDA-ODA PI parts.

cross-linkable polyimide precursor, polyamic diacrylate ester (PADE).<sup>6</sup> Leveraging VP to produce 3D parts, selective UV-irradiation of the PADE solution induced cross-linking of the acrylate groups and yielded an organogel. Subsequent drying and heating removed the solvent, promoted thermal degradation of the aliphatic cross-links, and converted the PADE to PMDA-ODA PI. Because of the rather time-consuming synthesis of PADE, we also successfully demonstrated photocurable PAA 2-(dimethylamino)ethyl methacrylate (DMAEMA) salt solutions as alternative photoresins for use in VP.<sup>7</sup> However, viscosity limitations imposed by VP restricted resin rheology, and thus solids loading of the polymer precursor.<sup>14,15</sup> To circumvent the viscosity constraints imposed by VP, afford the opportunity to print multiple materials in a single part, and reduce the amount of resin required to print, the authors look to direct ink write (DIW).

DIW is an additive manufacturing technique that selectively extrudes material by applying pressure to an ink, forcing it through a nozzle and onto a substrate to create a three-dimensional part.<sup>12</sup> For successful 3D printing via DIW, the material must be extrudable through a nozzle and, once deposited, rapidly solidify to retain its shape.<sup>12</sup> Several solidification mechanisms exist: (i) inks possessing a yield stress, meaning that the ink rapidly solidifies upon release of shear-stress,<sup>16</sup> (ii) solvent evaporation,<sup>17</sup> and (iii) gelation.<sup>18</sup> Ultraviolet-assisted direct ink write (UV-DIW) is a subcategory of DIW, which utilizes UV-irradiation to cross-link the extruded photopolymer resins during printing to induce gelation and shape retention after ink placement.<sup>19</sup> One advantage of UV-DIW over VP and inkjet material jetting AM processes is the ability to deposit a wide range of viscoelastic materials with viscosities in excess of 10 000 Pa s.<sup>14,16</sup> In addition, integration of multiple DIW systems into one printer enables simultaneous deposition of multiple materials into a single printed part, which enables manufacture of complex devices, such as soft robots and batteries.<sup>20,21</sup>

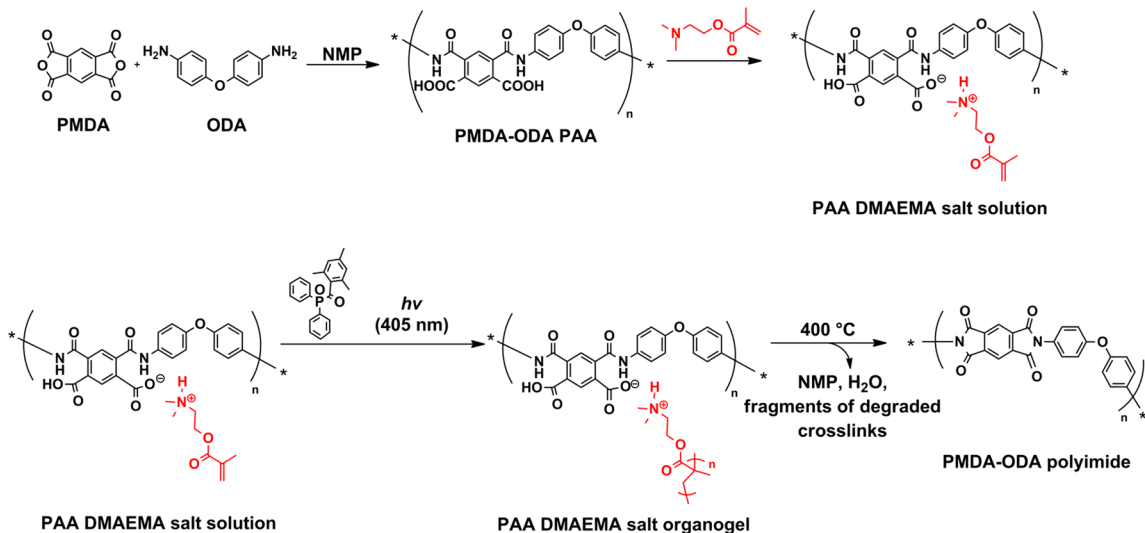
This work exploits UV-DIW to additively manufacture PMDA-ODA polyimide parts (Scheme 1). The tailored synthesis of a PAA 2-(dimethylamino)ethyl methacrylate (DMAEMA) salt solution yielded a UV-curable photoresin with a zero-shear rate viscosity of 770 Pa·s. The high photoreactive resin viscosity and shear thinning behavior enabled extrusion using DIW, and subsequent UV-irradiation to yield a self-supporting organogel. A short gel time and high gel state modulus enabled printing of freeform 3D structures

without need for support material. Finally, postprocess thermal treatment yielded PMDA-ODA PI with similar thermomechanical properties as commercial Kapton film.

Our recently developed strategy to AM PMDA-ODA PI using VP leveraged the solubility of PMDA-ODA polyamic acid (PAA).<sup>7</sup> The simple addition of an amino-functional methacrylate (DMAEMA) to a PAA solution rendered a photo-cross-linkable PAA DMAEMA salt solution (15 wt % PI solids), where the protonated DMAEMA interacted electrostatically with the partially deprotonated PAA. Selective layer-wise photocuring in VP system produced an organogel. Drying and heating released the solvent, promoted thermal degradation of the aliphatic cross-links and induced imidization to convert the organogel to the all-aromatic PMDA-ODA PI. The VP systems used required low solution viscosities of the resins, thus limiting their synthesis and formulation. In addition, the VP systems need a vat filled with resin, which increases the amount of material required and does not readily enable the deposition of multimaterial parts.

To enable the use of high viscosity resins, facilitate multimaterial printing, and reduce material usage, we explored UV-DIW as a printing technique. Similar to VP, UV-DIW required an ink with a short gel time, but contrary to VP, it demanded high solution viscosities and shear-thinning flow behavior. Utilizing the PAA DMAEMA salt strategy, one might have hypothesized that the simple increase in solids of the PAA solution would have afforded an ideal ink for UV-DIW. Intriguingly, this approach failed. The dissolution of PAA in NMP and addition of DMAEMA (0.5 equiv. per COOH) rendered a solution with 24 wt % PI solids, e.g., a solution with 9 wt % higher PI solids compared to the VP photoresin (Figure S1). Although the ink possessed a promising high zero-shear rate viscosity of 600 Pa·s and started to shear-thin at low shear rates ( $\sim 3 \text{ s}^{-1}$ ) (Figure S2), the ink suffered from slow photocuring characteristics. Photorheology elucidated that a solution with 10 wt % photoinitiator (TPO) possessed a rather long gel time ( $\sim 20 \text{ s}$ ) (Figure S3). Translated to the UV-DIW process, slow photocuring caused poor layer fidelity after ink deposition and precluded precise printing (Figure S4).

Instead of increasing the PI solid content of the ink, we leveraged the unusual solution viscosities of polyamic acids. The solution viscosities of PAAs depend strongly on their synthetic history. In particular, the viscosity of a PAA NMP solution is much higher if utilized directly after polymerization than if the PAA is precipitated from the reaction medium

Scheme 2. Ink Preparation Scheme<sup>a</sup>

<sup>a</sup>Step-growth polymerization of ODA and excess PMDA yielded a PMDA-ODA PAA with dianhydride end groups (indicated by the asterisk) in NMP. Addition of DMAEMA rendered the UV-curable ink. UV-illumination initiated crosslinking of DMAEMA and afforded an organogel. Drying and heating produced the all-aromatic PMDA-ODA PI and promoted thermal degradation of the PDMAEMA crosslinks.

(NMP) into a nonsolvent, filtered off, dried and redissolved. For example, step-growth polymerization of PMDA and ODA in NMP afforded a PAA with 16 wt % PI solids, which possessed an initial zero-shear rate solution viscosity of 270 Pa s. In contrast, after precipitation of the PAA in a methanol/water mixture, drying and redissolution in NMP, the viscosity of the PAA solution dropped to 0.9 Pa·s, which is more than two orders-of-magnitude lower (Figures S5 and S6). Although this phenomenon is still not fully understood, researchers have hypothesized that differences in PAA chain conformations in solution impart this change in viscosity.<sup>10</sup> In addition to differences in solution viscosity, the precipitated and redissolved PAA solution possessed an intensified amber color, which indicated partial imidization of the PAA due to drying at 60 °C. This complicated UV-DIW because the strong light absorbance of PMDA-ODA PI in the range of 200 to 500 nm hinders UV-absorbance of the photoinitiator and consequently impedes UV-initiation and cross-linking.<sup>22</sup>

The decreased UV-absorbance of nonisolated PAAs and their increased solution viscosities inspired exploitation of nonisolated PAAs as precursors for UV-DIW of polyimides. Step-growth polymerization of excess dianhydride (e.g., PMDA) and diamine (e.g., ODA) yielded a PAA with a targeted number-average molecular weight ( $M_n$ ) of 50 kg mol<sup>-1</sup> and dianhydride end groups (Scheme 2).

A representative nonisolated PAA solution (precursor) consisted of 17.8 wt % PI solids (Figure S7) and possessed a zero-shear rate viscosity of 330 Pa s. The addition of 0.5 equiv. of DMAEMA to the solution increased the viscosity further to 770 Pa s and pronounced the shear-thinning flow behavior, which reduced the pressure required for extrusion through a nozzle (Figure 1a). Addition of a typical UV-light photoinitiator (TPO) enabled UV-cross-linking of the DMAEMA groups. Because DMAEMA interacted electrostatically with the PAA backbone, UV-cross-linking of the DMAEMA induced gelation of the ink and afforded an organogel. Photorheology studies elucidated the gel state storage modulus ( $G'$ ) and gel time of the ink (Figure 1b). Varying the TPO amount and plotting the gel times versus wt % TPO indicated that 2.5 wt %

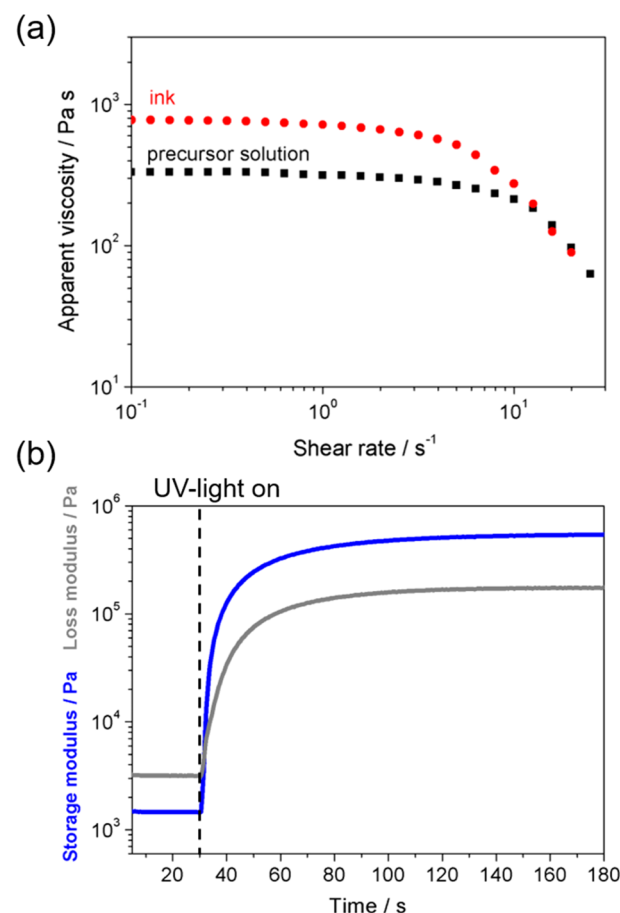
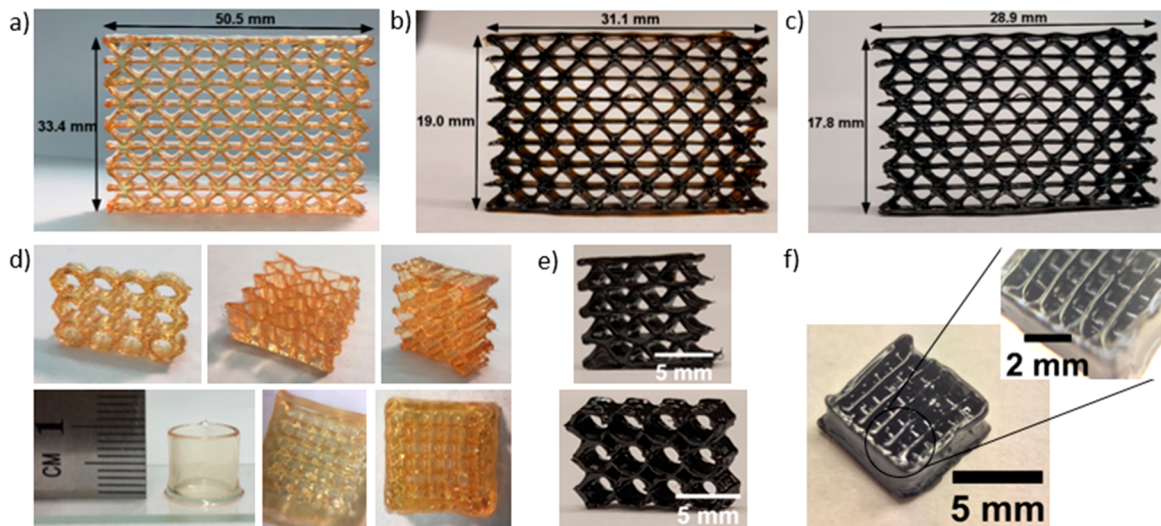


Figure 1. Data for a representative ink. (a) Apparent viscosity (Pa s) versus shear rate (s<sup>-1</sup>) for PAA in NMP (precursor) and PAA 0.5 equiv. DMAEMA salt solution (ink). (b) Moduli (Pa) versus time (s) from photorheology measurements of the PAA DMAEMA ink. UV-irradiation started at 30 s.

TPO was the minimum amount of photoinitiator to provide short gel times below 1.7 s (Figure S8 and Figure 1b). Fast



**Figure 2.** Photographs of (a) as-printed organogel part, (b) part dried at 200 °C in vacuum, (c) part after thermal imidization at 400 °C under nitrogen atmosphere. (d) As-printed organogel in various 3D geometries. (e) PMDA-ODA PI parts of various 3D geometries after imidization. (f) PMDA-ODA PI scaffold with self-supporting, bridging features after imidization.

gelation was crucial to solidify the printed lines in place after ink deposition. In addition, a high gel state modulus guaranteed shape retention of the deposited lines and allowed for printing of self-supporting structures.

A custom-built UV-DIW printer enabled AM of the ink (PAA DMAEMA salt solution). Deposition and subsequent UV curing of each layer yielded a self-supporting three-dimensional organogel that retained its shape even under the weight of subsequent layers (Figure 2a, d). Parts were printed using a nozzle with a diameter of 250  $\mu\text{m}$  that deposited lines averaging 500  $\mu\text{m}$  wide. Variation in deposition speed, extruder pressure, and layer height allowed for control over the deposited line width. An amber color UV-irradiation blocking syringe was used to prevent accidental curing and extended the pot life of the ink. The use of a polyethylene piston in the syringe body and the release of air trapped between the piston and photoresin reduced the photoresins exposure to air, minimizing cross-linking inhibition due to oxygen. The rather high zero-shear rate viscosity of the photoresin (770 Pa s), short curing times ( $\sim$ 1.7 s), and high gel state modulus ( $G' = 5 \times 10^5$  Pa), coupled with the geometric freedom provided by AM allowed printing of several complex structures, including cellular and truss structures with as-printed dimensions as large as 33.4 mm  $\times$  50.5 mm. Because DIW is not restricted to a printing stage submerged in a vat of material, larger structures are printable and would require significantly less material than VP.

Furthermore, fast gelation and mechanical integrity of the printed lines enabled AM of self-supporting features, with lines spanning gaps of 1.5 mm over the underlying layer. In particular, the print of simple cubic structures (SC-structures), evenly spaced parallel lines that were rotated by 90° every two layers, highlighted the self-supporting ability of the ink (Figure 2d). Figure 2f illustrates the final PMDA-ODA PI part, which demonstrate self-supporting bridges that retained their shape during imidization.

Removal of the cured organogel from the print substrate and subsequent hanging from a thin wire allowed for uniform evaporation of the solvent. A detailed drying and heating procedure removed all solvent, triggered thermal degradation

of the aliphatic cross-links (PDMAEMA) and induced imidization to afford the all-aromatic PI (Scheme 2). Solvent removal, pyrolysis of the PDMAEMA cross-links, and imidization induced an isotropic dimensional shrinkage of  $\sim$ 45%, which translated to a weight loss of  $\sim$ 83% and confirmed a PI solid loading of  $\sim$ 17% (Figure 2b, c, e, f).

The additively manufactured PMDA-ODA PI possessed a high thermal stability ( $T_{d,5\%} = 534$  °C), only slightly lower than a PI film prepared from commercial PAA ( $T_{d,5\%} = 550$  °C) (Figure 3a) using a doctor blade. High thermal stability is indispensable to enable applications for aerospace or military use. As illustrated in Figure 2, all PMDA-ODA PI objects possessed a darker color than commercial Kapton film. Although a darker color is expected because of the increased thickness of a printed structure (several mm) versus commercial thin film (30–50  $\mu\text{m}$ ), TGA measurements elucidated an increase in char yield of  $\sim$ 10 wt % of the AM specimen compared to commercial PI film. A higher char yield might indicate residual carbon in the AM PMDA-ODA PI due to the pyrolysis of the sacrificial PDMAEMA cross-links and photoinitiator. However, to date a more detailed analysis was unsuccessful.

Most importantly, dynamical mechanical analysis (DMA) of a printed AM specimen confirmed outstanding thermomechanical properties up to 400 °C, performing similarly to commercial Kapton film (Figure 3b). A storage modulus above 1 GPa up to 400 °C is essential to provide mechanical integrity to an AM part and enables potential applications over a wide temperature window.

In summary, UV-direct ink write enabled fabrication of complex 3D geometries of all-aromatic PMDA-ODA PI. PAA DMAEMA salt solutions served as UV-sensitive ink and yielded the PMDA-ODA PI upon heating and imidization. In particular, nonisolated PAA solutions provided the flow behavior needed for DIW extrusion. Extrusion and subsequent UV-illumination allowed for printing arbitrary shapes, e.g., truss and cellular structures. The short gel times of the PAA DMAEMA ink and high gel state modulus of the organogel enabled printing of self-supporting SC-structures, with lines spanning gaps of 1.5 mm in the underlying layer. Drying and

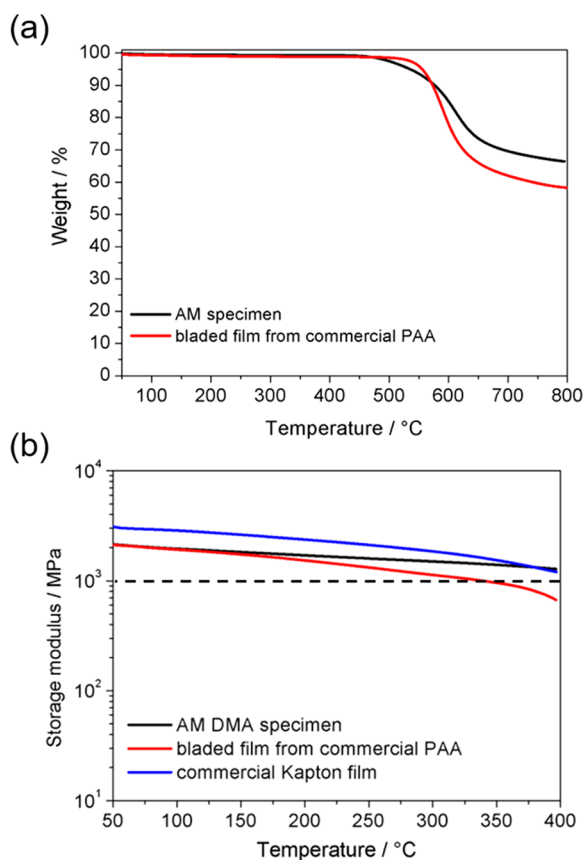


**Figure 3.** (a) TGA traces of AM specimen and bladed film from commercial PAA after imidization. (b) Storage modulus (MPa) versus temperature (°C) for AM specimen, bladed film from commercial PAA after imidization and commercial Kapton film.

heating of the 3D parts removed solvent, promoted thermal degradation of the sacrificial cross-links, and induced imidization. Although the thermal treatment resulted in 45% isotropic dimensional shrinkage and might complicate the production of complex features, part fidelity was maintained. TGA and DMA measurements demonstrated high thermal stability and good mechanical strength of 3D printed parts up to +400 °C. Increased char yields of the AM PI indicated residual carbon due to pyrolysis of the PDMAEMA cross-links and photoinitiator. A more detailed analysis of the char formation and potential residual carbon in the PI is under investigation. Overall, UV-DIW of PAA DMAEMA ink possesses potential for future multimaterial 3D printing of components that are resistant to solvents, extreme temperatures, and radiation.

## ASSOCIATED CONTENT

### Supporting Information

The Supporting Information is available free of charge on the ACS Publications website at DOI: [10.1021/acsami.8b14584](https://doi.org/10.1021/acsami.8b14584).

Experimental part and additional data ([PDF](#))

## AUTHOR INFORMATION

### Corresponding Author

\*E-mail: [cwill@vt.edu](mailto:cwill@vt.edu).

ORCID iD

Daniel A. Rau: 0000-0002-3112-954X

Timothy E. Long: [0000-0001-9515-5491](https://doi.org/0000-0001-9515-5491)

### Author Contributions

†D.A.R. and J.H. contributed equally to this work.

### Notes

The authors declare no competing financial interest.

## ACKNOWLEDGMENTS

The authors graciously acknowledge RJ Reynolds, Winston Salem, North Carolina, USA, for financial support. The authors acknowledge Ryan Mondschein of the Long Research Group for useful discussions regarding solution rheology measurements. The authors also acknowledge Viswanath Meenakshisundaram and Nicholas A. Chartrain of the DREAMS lab for valuable discussions on the additive manufacturing of organogels.

## REFERENCES

- Huang, Y.; Leu, M. C.; Mazumder, J.; Donmez, A. Additive Manufacturing: Current State, Future Potential, Gaps and Needs, and Recommendations. *J. Eng. Ind.* **2015**, *137*, 014001.
- Gao, W.; Zhang, Y.; Ramanujan, D.; Ramanan, K.; Chen, Y.; Williams, C. B.; Wang, C. C.; Shin, Y. C.; Zhang, S.; Zavattieri, P. D. The Status, Challenges, and Future of Additive Manufacturing in Engineering. *Comput.-Aided Des.* **2015**, *69*, 65–89.
- Deng, D.; Chen, Y.; Zhou, C. Investigation on PEEK fabrication using Mask-image-projection-based Stereolithography, *Solid Freeform Fabr. Symp. Proc.*, **2012**, 606–616.
- Kishore, V.; Chen, X.; Ajinjeru, C.; Hassen, A. A.; Lindahl, J.; Faila, J.; Kunc, V.; Duty, C. Additive Manufacturing of High Performance Semi-crystalline Thermoplastics and Their Composites. *Solid Freeform Fabr. Symp. Proc.* **2016**, 906–915.
- Bagsik, A.; Schöppner, V.; Klemp, E. FDM Part Quality Manufactured With Ultem® 9085. *Int. Sci. Conf. Polym. Mater.* **2010**, 307–315.
- Hegde, M.; Meenakshisundaram, V.; Chartrain, N.; Sekhar, S.; Tafti, D.; Williams, C. B.; Long, T. E. 3D Printing All-Aromatic Polyimides using Mask-Projection Stereolithography: Processing the Nonprocessable. *Adv. Mater.* **2017**, *29*, 1701240.
- Herzberger, J.; Meenakshisundaram, V.; Williams, C. B.; Long, T. E. 3D Printing All-Aromatic Polyimides Using Stereolithographic 3D Printing of Polyamic Acid Salts. *ACS Macro Lett.* **2018**, *7*, 493–497.
- Zhang, F.; Tuck, C.; Hague, R.; He, Y.; Saleh, E.; Li, Y.; Sturgess, C.; Wildman, R. Inkjet Printing of Polyimide Insulators for the 3D Printing of Dielectric Materials for Microelectronic Applications. *J. Appl. Polym. Sci.* **2016**, *133*, 43361.
- <http://www.dupont.com/content/dam/dupont/products-and-services/membranes-and-films/polyimide-films/documents/DEC-Kapton-summary-of-properties.pdf> Accessed February 3, 2018.
- Wilson, D.; Stenzenberger, H. D.; Hergenrother, P. M. *Polyimides*; Springer: 1990.
- Bershtean, V.; Sukhanova, T.; Krizan, T.; Keating, M.; Grigoriev, A.; Egorov, V.; Yakushev, P.; Peschanskaya, N.; Vylegzhannina, M.; Bursian, A. Relationship of Processing Conditions to Structure and Properties in PMDA-ODA Polyimide. *J. Macromol. Sci., Part B: Phys.* **2005**, *44*, 613–639.
- Gibson, I.; Rosen, D. W.; Stucker, B. *Additive Manufacturing Technologies*; Springer: 2010; Vol. 238.
- Fukukawa, K.-i.; Ueda, M. Recent progress of photosensitive polyimides. *Polym. J.* **2008**, *40*, 281.
- Vaezi, M.; Seitz, H.; Yang, S. A Review on 3D Micro-additive Manufacturing Technologies. *Int. J. Adv. Manuf. Technol.* **2013**, *67*, 1721–1754.
- Bártolo, P. J. *Stereolithography: Materials, Processes and Applications*; Springer Science & Business Media: 2011.
- Compton, B. G.; Lewis, J. A. 3D-printing of Lightweight Cellular Composites. *Adv. Mater.* **2014**, *26*, 5930–5935.

- (17) Guo, S. Z.; Gosselin, F.; Guerin, N.; Lanouette, A. M.; Heuzey, M. C.; Therriault, D. Solvent-cast three-dimensional printing of multifunctional microsystems. *Small* **2013**, *9*, 4118–4122.
- (18) Gratson, G. M.; Lewis, J. A. Phase Behavior and Rheological Properties of Polyelectrolyte Inks for Direct-write Assembly. *Langmuir* **2005**, *21*, 457–464.
- (19) Lebel, L. L.; Aissa, B.; Khakani, M. A. E.; Therriault, D. Ultraviolet-Assisted Direct-Write Fabrication of Carbon Nanotube/Polymer Nanocomposite Microcoils. *Adv. Mater.* **2010**, *22*, 592–596.
- (20) Schaffner, M.; Faber, J. A.; Pianegonda, L.; Rühs, P. A.; Coulter, F.; Studart, A. R. 3D Printing of Robotic Soft Actuators with Programmable Bioinspired Architectures. *Nat. Commun.* **2018**, *9*, 878.
- (21) Sun, K.; Wei, T. S.; Ahn, B. Y.; Seo, J. Y.; Dillon, S. J.; Lewis, J. A. 3D Printing of Interdigitated Li-Ion Microbattery Architectures. *Adv. Mater.* **2013**, *25*, 4539–4543.
- (22) Virk, H.; Chandi, P.; Srivastava, A. Physical and Chemical Response of 70 MeV Carbon Ion Irradiated Kapton-H Polymer. *Bull. Mater. Sci.* **2001**, *24*, 529–534.